buildings

MDPI

Article

Characterization of Buriti (*Mauritia flexuosa)* Foam for Thermal Insulation and Sound Absorption Applications in Buildings

Felippe Fabrício dos Santos Siqueira [1,2,*], Renato Lemos Cosse [3], Fernando Augusto de Noronha Castro Pinto [4], Paulo Henrique Mareze [5], Caio Frederico e Silva [6] and Lívio César Cunha Nunes [1,7]

1 Graduate Program in Materials Science and Engineering, Technology Center, Federal University of Piauí, Teresina 64049-550, PI, Brazil; liviocesar@ufpi.edu.br
2 Federal Institute of Education, Science and Technology of the Sertão Pernambucano, Ouricuri 56302-100, PE, Brazil
3 Macromolecular Chemistry & New Polymeric Materials, Zernike Institute for Advanced Materials, University of Groningen, 9712 CP Groningen, The Netherlands; r.lemos.cosse@rug.nl
4 Laboratory of Acoustics and Vibrations (LAVI), Graduate Program in Mechanical Engineering, Technology Center, Federal University of Rio de Janeiro, Rio de Janeiro 21941-901, RJ, Brazil; fcpinto@ufrj.br
5 Acoustic Engineering, Federal University of Santa Maria, Santa Maria 97105-900, RS, Brazil; paulo.mareze@eac.ufsm.br
6 Graduate Program in Architecture and Urbanism, Faculty of Architecture and Urbanism, University of Brasília, Brasília 70910-900, DF, Brazil; caiosilva@unb.br
7 Graduate Program in Intellectual Property and Technology Transfer (PROFNIT), Federal University of Piauí, Teresina 64049-550, PI, Brazil
* Correspondence: felippe.fabricio@ifsertao-pe.edu.br

Abstract: Exploring new construction materials with low environmental impact leads to innovation in buildings and also to the expansion of environmental sustainability in the construction industry. In this perspective, the thermal insulation and the sound absorption performances of Buriti (Mauritia flexuosa) foam were analyzed for potential application in buildings. This material is of plant origin, it is natural, renewable, abundant, and has a low environmental impact. In this research, characterizations were made by scanning electron microscopy (SEM), apparent density, thermogravimetry (TGA and DTG), thermal conductivity, and sound absorption. The SEM analysis revealed a predominantly porous, small, and closed-cell morphology in the vegetable foam. Due to its porosity and lightness, the material has an apparent density similar to other thermal insulating and sound-absorbing materials used commercially. The evaluation of thermogravimetric (TGA/DTG) results demonstrated thermal stability at temperatures that attest to the use of Buriti foam as a building material. Based on the thermal conductivity test, the Buriti foam was characterized as an insulating material comparable to conventional thermal insulation materials and in the same range as other existing thermal insulators of plant origin. Concerning sound absorption, the Buriti foam presented a low performance in the analyzed frequency range, mainly attributed to the absence of open porosity in the material. Therefore, understanding the sound absorption mechanisms of Buriti foam requires further studies exploring additional ways of processing the material.

Keywords: thermal conductivity; acoustic materials; natural resources; environmental sustainability; sustainable building materials

Citation: Siqueira, F.F.S.; Cosse, R.L.; Pinto, F.A.N.C.; Mareze, P.H.; Silva, C.F.; Nunes, L.C.C. Characterization of Buriti (*Mauritia flexuosa)* Foam for Thermal Insulation and Sound Absorption Applications in Buildings. *Buildings* **2021**, *11*, 292. https://doi.org/10.3390/buildings11070292

Academic Editors: João Gomes Ferreira and Ana Isabel Marques

Received: 30 May 2021
Accepted: 1 July 2021
Published: 5 July 2021

1. Introduction

Buildings are one of the main factors behind the environmental impacts of human activities. One way of attempting to reduce these negative impacts and guarantee the sustainable development of the construction industry is to seek new materials and construction systems whose components are of a renewable origin and have a low energy cost of production and application, including low emission of pollutants during their production [1–3].

Among the various materials employed in the construction market, attention can be drawn to the traditional thermal insulators and sound absorbers, which are generally produced either with non-renewable synthetic materials of fossil origin or with materials from natural resources processed with high energy consumption. In addition, they are expensive to produce and have several negative implications for the environment [4–8].

In an attempt to overcome these drawbacks, many researchers have been working on replacing these building materials with natural, renewable, and recycled options to limit greenhouse gas emissions, conserve natural resources, and improve the environmental performance of buildings [6–12]. Khalaf et al. [13] investigated the use of miscanthus, recycled textile, and rice husks as reinforcement for the chitosan matrix to produce new insulating composites for building application. The authors concluded that the formulations with small size miscanthus have potential and competitive application compared to conventional insulating materials. Mrajji et al. [14] developed a new insulation material based on chicken feathers waste. The results of the study showed low thermal conductivity values, being a good candidate for use as a low-cost, environmentally friendly insulation material in constructions. Caniato et al. [15] studied the thermal and acoustic properties of an innovative open-cell foam produced using a bio-based matrix and incorporating microplastic waste. Besides the composites work as an alternative application for disposable plastics, they performed as candidates for replacing current sound absorbers and thermal insulators.

Regarding new approaches to building designs, the development and use of natural and local building materials are gaining strength [16]. In this category, fibrous and porous materials of plant origin are increasingly finding applications in the construction industry due to their low density, low embodied energy, economy, and environmental sustainability [3–7,17]. They are widely available in nature, present no damage to health, have low cost, and are renewable and recyclable [1,3,5,7,18]. Furthermore, the transformation process of these materials into a final product also involves fewer steps and requires less energy than petrochemical or mineral materials [4]. However, many of the properties of these natural materials are still underexplored or unknown.

Fibrous materials consist of a series of tunnel-like openings formed by interstices between the bulk material's fibers, while porous materials comprise numerous cellular structures or gaps. Due to the low density deriving out of the significant presence of enclosed air in their structures, materials with these characteristics are widely used as thermal insulators and sound absorbers in buildings [3].

Among the materials of plant origin with such characteristics and with exploitation potential in Brazil, the natural foam obtained from the Buriti palm (*Mauritia flexuosa*) stands out. The Buriti is a robust palm tree with large leaves arranged in a fan shape [19]. It is native to the Amazon and Cerrado biomes, spreading especially over the North and Northeast regions of the Brazilian territory. It is one of the most common and abundant palm trees in the country, growing in the immense form of homogeneous populations in swampy places [19–22]. The petiole of the Buriti leaf is internally comprised of thin and aligned fibers surrounded by a light color, lightweight, and a relatively soft porous vegetable tissue (Buriti foam). In its outer part, the petiole is composed of a rigid bark that protects the vegetable foam.

Culturally, the Buriti palm is used in several ways. The leaf petiole is used in the manufacture of furniture and decorative objects. The straw is used to cover houses, as well as in the artisanal production of various products. Its fruits are used for the production of sweets, juices, and liqueurs. The oil extracted from the fruits has medical applications and is rich in vitamin A, making it suitable to produce cosmetics [20]. Despite its numerous applications, there are few scientific studies on this palm, especially regarding its use in buildings.

In light of the information exposed above, it is safe to assume that the use of the natural Buriti foam has promising potential to promote thermal insulation and sound absorption in buildings. The abundance of this palm in the Brazilian territory, associated

with the intrinsic characteristics of the vegetable foam, arouses scientific and commercial interest in its use for substituting its synthetic pairs.

In this sense, this research aims to analyze the performance of thermal insulation and sound absorption of Buriti foam for building applications. For this purpose, characterizations were performed by scanning electron microscopy (SEM), apparent density, thermogravimetry (TGA/DTG), thermal conductivity, and sound absorption.

2. Materials and Methods

2.1. Materials

As a way of stimulating and intensifying the use of regional materials in buildings, this research relied on using the Buriti foam in nature obtained from palm trees native to the city of Caxias, Maranhão, in the Northeast of Brazil. The vegetable foam was extracted from the petioles of adult and dry leaves that later regenerate naturally, without harming the environment. Figure 1 shows the petiole of the Buriti leaf.

(**a**) (**b**) (**c**)

Figure 1. Buriti foam: (**a**) palm leaves with red arrows highlighting the petiole from which the vegetable foam is taken, (**b**) petiole longitudinal section, and (**c**) petiole cross-section.

After the removal of the petioles, they were ready for the extraction of the vegetable foam. First, the petioles were cut into sizes of approximately one meter in length. Then, the barks were removed, leaving the Buriti foam exposed. Finally, the foams were cut into layers of various thicknesses to be used in the production of specimens for further characterizations and analysis. Figure 2 illustrates the schematic process for preparing the Buriti foam.

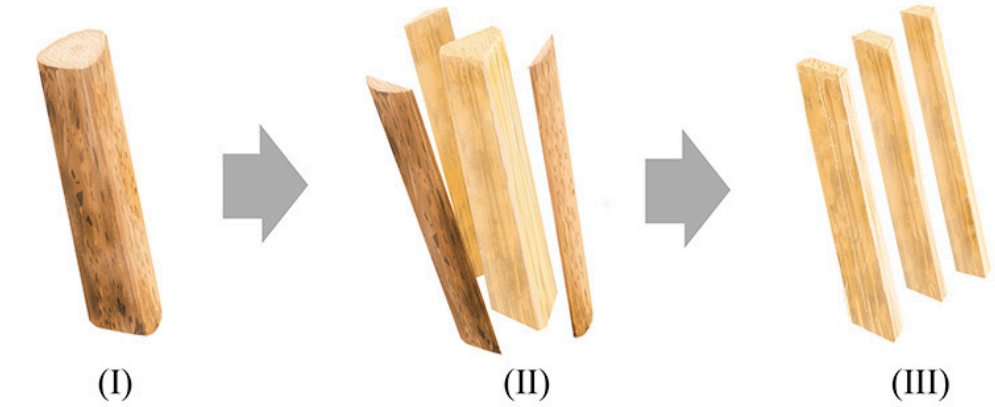

Figure 2. Schematic process of preparing the Buriti foam: (**I**) petiole cutting, (**II**) removal of the bark leaving the Buriti foam exposed, and (**III**) lamination of the Buriti foam.

The PVA Cascola Cascorez Extra® adhesive was used for bonding the Buriti foam boards to be used for the sound absorption test. The adhesive is a water-based material with high bond strength, free of solvents, and without toxic characteristics. Figure 3 illustrates the Buriti foam boards production process.

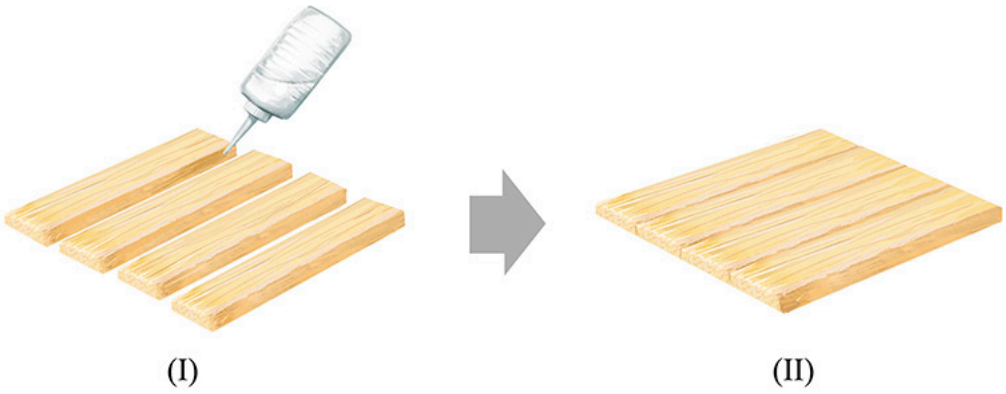

Figure 3. Buriti foam boards production: (**I**) bonding the layers of Buriti foam with the PVA adhesive, and (**II**) Buriti foam board.

In this research, expanded polystyrene (EPS) worked as a reference in the experimental test to measure the thermal conductivity of Buriti foam. The EPS used was the Isopor® manufactured by Knauf. Table 1 describes some properties of the material.

Table 1. Properties of EPS Isopor®.

Properties	EPS Isopor®
Apparent density (kg/m^3)	14
Thermal Conductivity (W/mK)	0.042
Flammability	Flame resistant

2.2. Characterizations and Tests

2.2.1. Morphological Characterization

The characterization by scanning electron microscopy (SEM) was conducted to investigate the morphology and the structure of the Buriti foam. The image analyses were conducted on both the longitudinal and the transverse surfaces. The samples were fixed on brass stubs with carbon tape and previously coated with a thin layer of gold employing

the Quorum Q150R metallizer. The micrographs were performed by the JEOL JSM-IT300 equipment in a high vacuum in the secondary electron detection mode, under 10 kV voltage.

2.2.2. Apparent Density Test

The Buriti foam apparent density test was conducted according to the recommendations of the ASTM D1622 standard [23]. Samples in the cubic format of $3 \times 3 \times 3$ cm^3 from three different palm petioles were considered. The test was carried out using three samples of vegetable foam in natura from each palm, for a total of nine measurements, with the intent of reaching a more precise apparent density for the material.

The mass and the volume of the samples were measured using an analytical balance with a 0.0001 g accuracy and a metallic digital caliper respectively. The apparent density of the samples was calculated through Equation (1):

$$D = \frac{W_s}{V}, \quad (1)$$

where D is the apparent density (kg/m^3), W_s is the sample weight (kg) and V is the sample volume (m^3).

2.2.3. Thermogravimetric Characterization (TGA/DTG)

Thermogravimetric analysis is a destructive test that evaluates mass variation as a function of temperature. The thermal degradation events of the Buriti foam were studied to evaluate its heat resistance and its operating limit temperature as a building material.

The test was performed using the TA Instruments Q600 SDT equipment with detection sensitivity in the mass variation of 0.1 µg and 0.001 °C of temperature, with an accuracy of ±2%. Approximately 2 mg of the material was heated from room temperature up to 700 °C with a gas flow of 50 mL/min, at a heating rate of 10 °C/min, in an inert argon (Ar) atmosphere.

2.2.4. Thermal Conductivity Test

As a way of assessing the conductivity of the Buriti foam, a comparative experimental procedure was adopted. The test assembly is shown in Figure 4.

The equipment configuration followed a few steps. First, the power supply was calibrated to a 0.4 A current that generated a corresponding 4.8 V voltage. Then, the thermoelectric cooler was connected to the power supply. After that, the 40×40 mm^2 sized and 5 mm thick sample was placed on the hot surface of the thermoelectric cooler.

To collect temperature variations, two type K thermocouples were connected to a data logger. One of the thermocouples was placed between the hot surface of the thermoelectric cooler and the lower surface of the sample and the other on the upper surface, with the use of thermal tape for fixation. The entire assembly was fixed on the bench vise. Before the start of the test, the samples were previously oven-dried for 4 h at 70 °C.

The ambient temperature was controlled at around 24 °C, and the relative humidity of the air was approximately 55%. The temperatures on the two thermocouples were monitored during heating at one-second intervals. After the necessary time had elapsed, the power supply was turned off and the temperatures were additionally collected during cooling until they reached the same value in the two thermocouples.

According to Kreith, Manglik, and Bohn [24], heat flows from the highest to the lowest temperature region whenever there is a temperature gradient in a solid medium. The rate of heat flow transferred by conduction between the two surfaces, as in the experiment, can be governed by the Fourier Conduction Law. When the conduction heat transmission has a constant heat flow through a flat wall, its fundamental relationship is defined by Equation (2):

$$q_k = \frac{\lambda \, \Delta T}{L}, \quad (2)$$

where q_k is the heat flow (W/m^2), λ is the thermal conductivity of the material (W/mK), ΔT is the temperature difference between the sample surfaces (K), and L is the sample thickness (m).

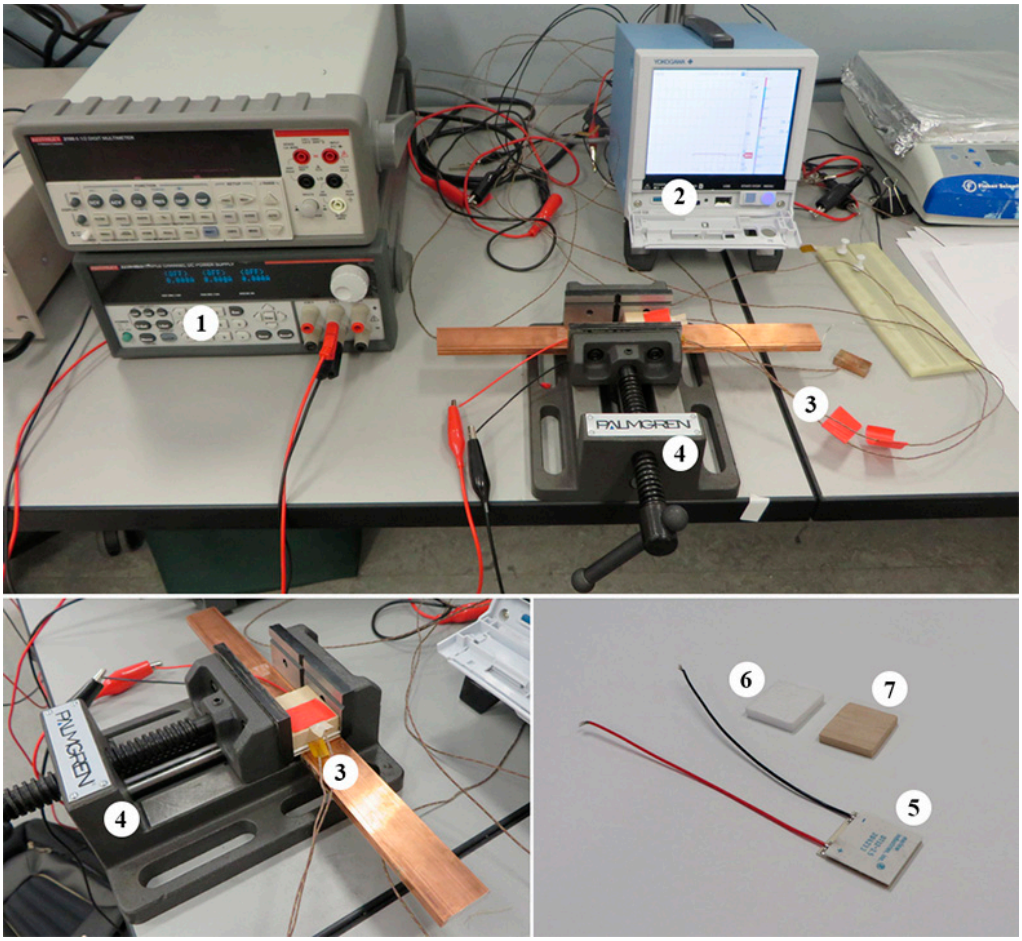

Figure 4. Thermal conductivity test assembly and equipment: 1—Power supply (Keithley 2230), 2—Datalogger (Yokogawa G10), 3—Thermocouple (Type K), 4—Bench vise (Palmgren), 5—Thermoelectric cooler (Marlow Industries DT12-2.5), 6—EPS sample (Knauf Isopor®), and 7—Buriti foam sample.

Before proceeding with measuring the thermal conductivity of the Buriti foam, the experimental procedure was performed first for the EPS sample. The experiment used this material as a comparative reference because it is a good thermal insulator, with thermal properties already known and cataloged. From the test, it was possible to monitor the temperature variation on the upper and lower surfaces of the EPS sample. Applying Equation (2), it was possible to calculate the heat flow (q_k) through the EPS sample.

The same procedure was carried out on three samples of the Buriti foam. Since the parameters adopted were the same, the heat flow supplied to the EPS sample can be considered equal to that supplied to the Buriti foam samples. Thus, by applying Equation (2) again, the thermal conductivity value (λ) of the Buriti foam was experimentally obtained.

2.2.5. Sound Absorption Test

The procedure for measuring the sound absorption of Buriti foam considered the ASTM E1050 [25] and ISO 10534-2 [26] standards that regulate the measurement of the normal incidence absorption coefficients in an impedance tube using the two-microphone method. The assembly and equipment used in the sound absorption test are shown in Figure 5.

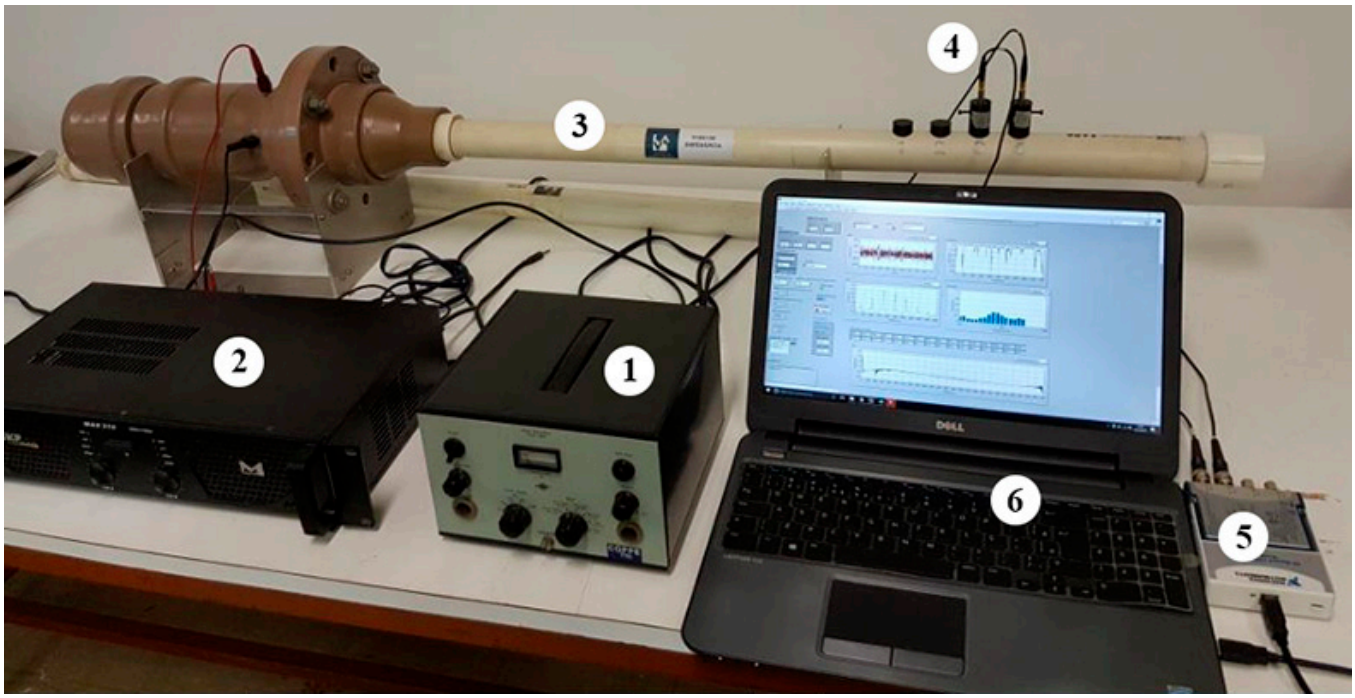

Figure 5. Sound absorption test assembly and equipment: 1—Signal generator (B&K 1405), 2—Power Amplifier (SKP MAX 310), 3—Impedance Tube (LAVI/UFRJ), 4—Microphones (BSWA MPA416 1/4"), 5—Signal Processor Board (NI 9234) and 6—Processing Software (LabVIEW).

The impedance tube was designed and built at the Laboratory of Acoustics and Vibrations of the Federal University of Rio de Janeiro (LAVI/UFRJ). The distance between the microphones, the diameter of the tube and the speed of sound inside it allowed measurements in third-octave bands in the frequency range of 100 to 3150 Hz. This is a representative range of sound which includes a large part of what is assimilated by the human ear [7].

The experiment was carried out in four configurations of Buriti foam, in thicknesses of 15 mm and 25 mm, both in the longitudinal (BFL) and in the transverse (BFT) cutting directions, as shown in Table 2. The test was performed on three samples for each configuration.

Table 2. Configurations of Buriti foam samples.

Sample Configuration	Cutting Direction	Thickness (mm)
BFL-15	Longitudinal	15
BFL-25	Longitudinal	25
BFT-15	Transverse	15
BFT-25	Transverse	25

The samples used were laser cut with a 45 mm diameter from boards produced with layers of Buriti foam, as shown in Figure 6.

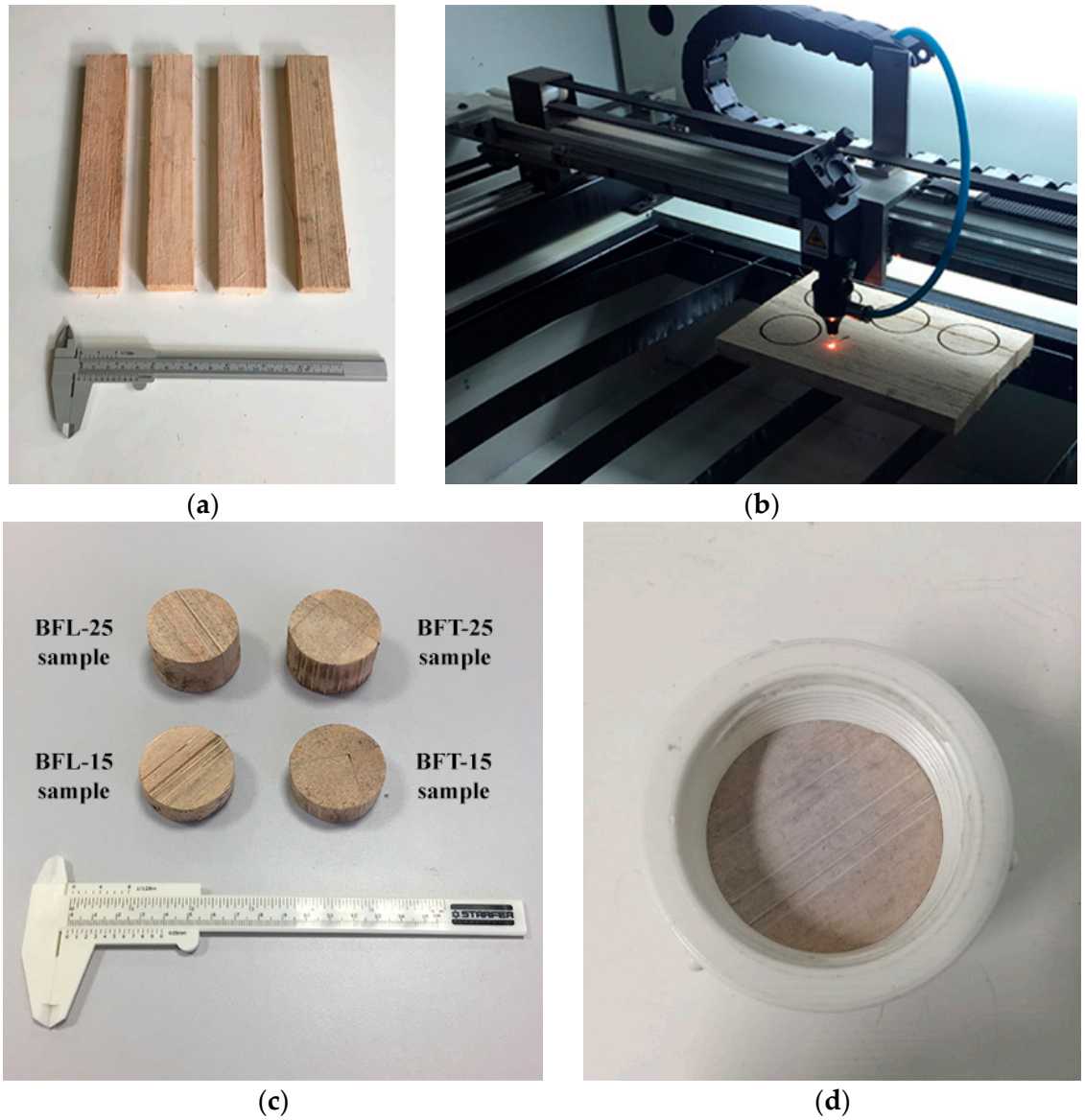

Figure 6. Buriti foam samples for the sound absorption test: (**a**) layers of Buriti foam for boards production, (**b**) laser cutting of the samples, (**c**) longitudinal and transverse configurations of the Buriti foam samples, and (**d**) Buriti foam sample inside the sample holder of the impedance tube.

Given that the aim is to characterize only the effects of the material, no air space was used behind the samples. In addition, care was taken to avoid spaces between the sample and the tube walls.

3. Results and Discussion

3.1. Morphological Characterization

The SEM micrographs of the Buriti foam, both on the longitudinal and the transverse surface, are shown in Figure 7.

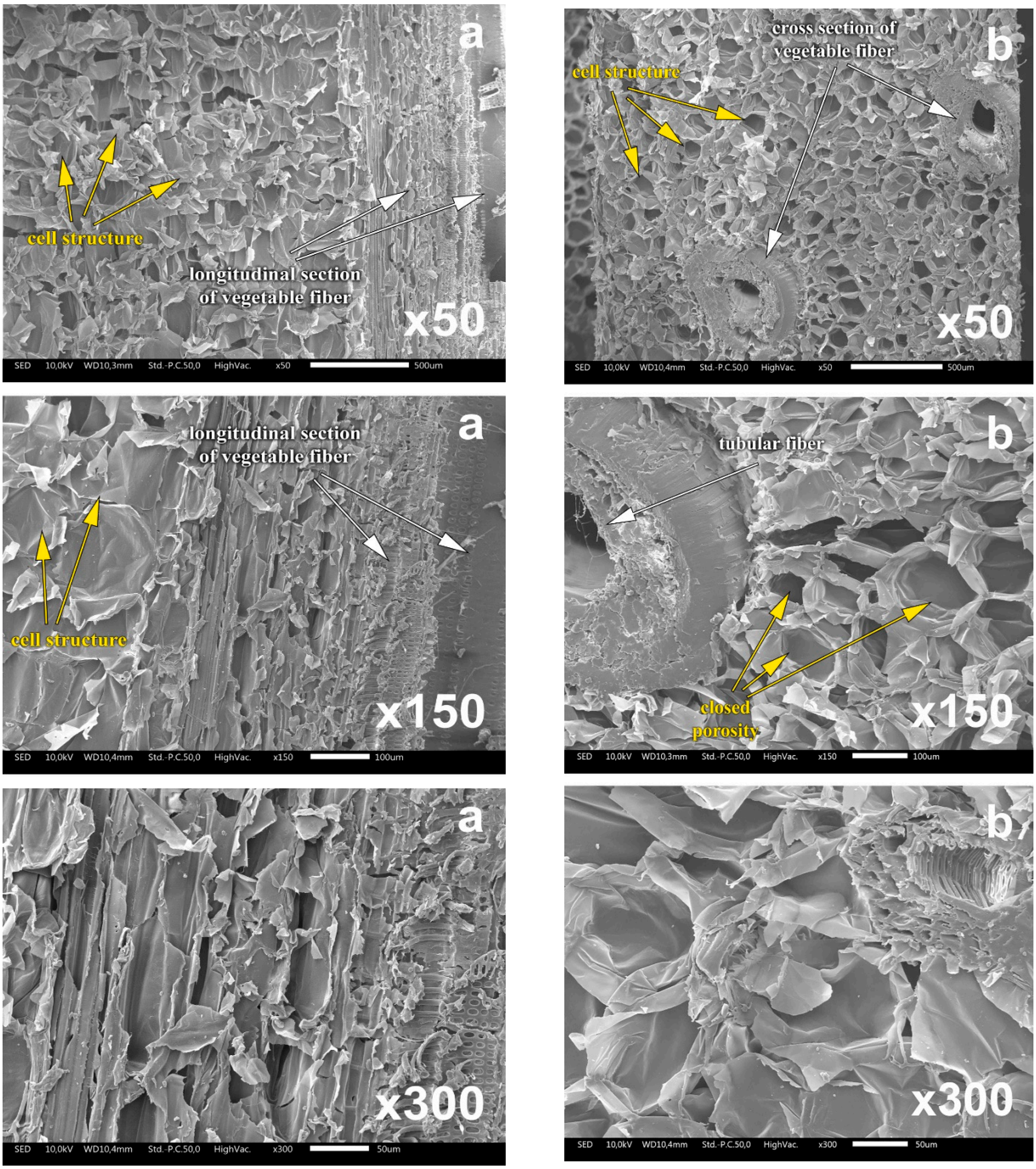

(**a**) (**b**)

Figure 7. SEM micrographs of Buriti foam with magnifications of ×50, ×150, and ×300: (**a**) longitudinal surface and (**b**) transverse surface.

In general, the micrographs showed that the Buriti foam has a predominantly porous structure involving thin fibers distributed inside the material.

From Figure 7a, two characteristics can be observed on the longitudinal surface of the Buriti foam: a more irregular region that corresponds to the cellular structure of the vegetable tissue, and another, slightly more uniform, that refers to the longitudinal section of the vegetable fiber present inside the porous structure. This aspect is highlighted in Figure 7b, which represents the transverse surface of the material. It is noticeable that the cellular structures are closed, bounded by thin, randomly oriented walls. The cell dimensions are not uniform, with the cell diameter being much larger than the wall

thickness, ranging from approximately 60 to 150 µm. For comparative purposes, the cell size of expanded polystyrene (EPS) foam averages 80 to 150 µm [6].

The micrographs of the transverse surface, also depict the fibers involved in the cellular structure of the vegetable tissue. The fibers have a tubular shape, a diameter around 500 to 700 µm, and a wall thickness that reaches 280 µm. According to Cardoso and Gonçalez [27], the presence of these fibers contributes to increasing the mechanical resistance of the Buriti foam.

From the thermal insulation point of view, closed porosity is generally beneficial due to the presence of still air inside the material cavities [28]. In general, materials with tiny and closed pores tend to have a lower thermal conductivity than those with large or open pores [29].

On the other hand, although porous sound-absorbing materials are generally good thermal insulators, the reverse is not always true. Sound absorbing materials require air circulating inside, so open porosity is essential [28].

3.2. Apparent Density Test

The results of the apparent density test are shown in Table 3 and Figure 8.

Table 3. Measurements of weight and apparent density of Buriti foam samples.

	Sample	Weight	Apparent Density
Palm Tree A	1	1.1556 g (1.1556×10^{-3} kg)	0.04280 g/cm^3 (42.80 kg/m^3)
	2	1.1440 g (1.1440×10^{-3} kg)	0.04237 g/cm^3 (42.37 kg/m^3)
	3	1.1358 g (1.1358×10^{-3} kg)	0.04207 g/cm^3 (42.07 kg/m^3)
Palm Tree B	1	1.3599 g (1.3599×10^{-3} kg)	0.05037 g/cm^3 (50.37 kg/m^3)
	2	1.3401g (1.3401×10^{-3} kg)	0.04963 g/cm^3 (49.63 Kg/m^3)
	3	1.3272 g (1.3272×10^{-3} kg)	0.04916 g/cm^3 (49.16 kg/m^3)
Palm Tree C	1	1.5019 g (1.5019×10^{-3} kg)	0.05563 g/cm^3 (55.63 kg/m^3)
	2	1.5197 g (1.5197×10^{-3} kg)	0.05629 g/cm^3 (56.29 kg/m^3)
	3	1.5742 g (1.5742×10^{-3} kg)	0.05608 g/cm^3 (56.08 kg/m^3)

As seen in the results, the Buriti foam samples from the three palms had different apparent density values. This indicates a difference in enclosed air in the samples of vegetable foam from the three palms. According to Li and Ren [29], materials with lower apparent density also have greater porosity. Thus, it can be inferred that the Buriti foam from palm A has a higher porosity than the vegetable foams from palm B and C, which explains the different apparent density values found.

Regarding the general apparent density measurement of the Buriti foam (palm trees A, B, and C), the high standard deviation seen in Figure 8 confirms the heterogeneity of the vegetable foam. This is considered normal when it comes to natural materials. According to Berardi and Iannace [3], porous materials of vegetal origin present a greater heterogeneity in their morphology when compared to synthetic porous ones.

The average apparent density for the Buriti foam was 49.38 ± 5.9 kg/m^3. This value results from the cellular morphology of the vegetable foam which, due to its predominantly porous characteristic, contributed to its low density [30,31]. The literature reports that the apparent density of Buriti foam is not very different from conventional materials, such as

rock wool, fiberglass, expanded polystyrene (EPS), and polyurethane foam (PUR), whose densities can vary, respectively, between 40–200 kg/m^3, 15–75 kg/m^3, 15–35 kg/m^3 and 15–45 kg/m^3 [28,32].

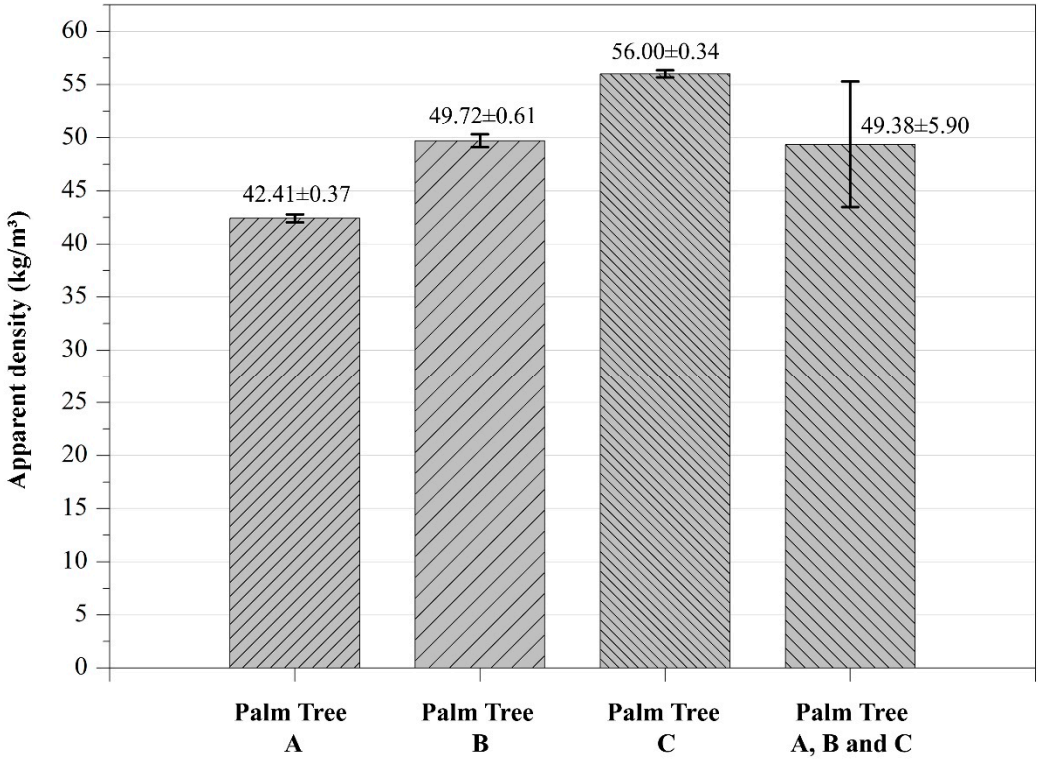

Figure 8. Apparent density of Buriti foam.

3.3. Thermogravimetric Characterization (TGA/DTG)

The TGA and DTG thermogravimetric curves for Buriti foam in an inert argon (Ar) atmosphere are illustrated in Figure 9.

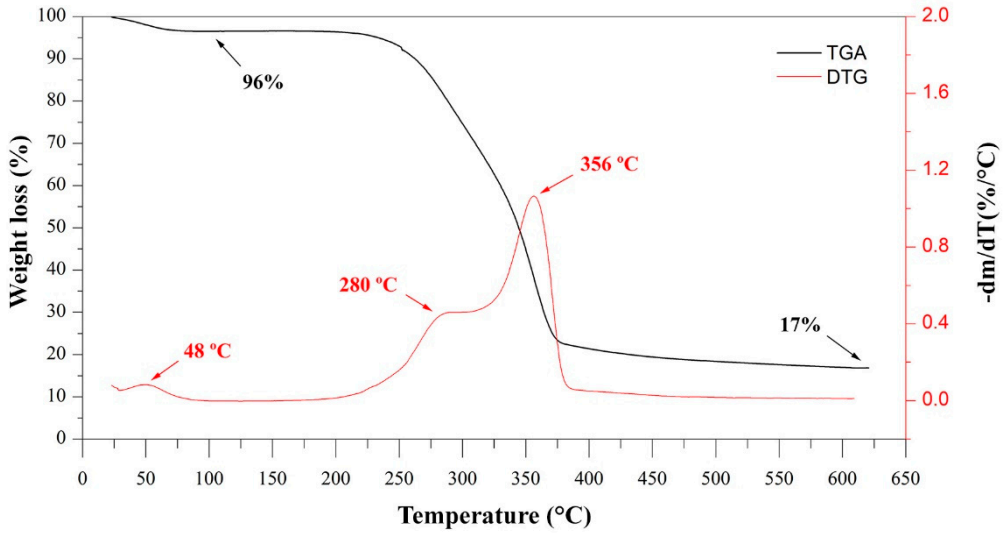

Figure 9. TGA and DTG curves for the Buriti foam.

The TGA curve shows the thermal decomposition process of Buriti foam. Initially, a 4% loss of mass is observed up to 100 °C, normally attributed to the evaporation of the water present in the lignocellulosic structure [33–36].

After this stage, the curve remains at a stable level up to 180 °C. Subsequently, at this temperature, the sample showed different stages of mass loss associated with events of thermal degradation of the plant structure through the rupture of its macromolecular chains [37]. The sample decomposed up to about 600 °C, representing an increase in mass loss of approximately 79%.

At the end of the thermal decomposition process, the sample goes through a second stable level with a residual mass value of around 17%. According to Souza et al. [34], these residues are probably related to inert ash and metallic oxides formed from the minerals present in the vegetable foam that have not decomposed.

The results show that the thermal decomposition of the material occurred through three thermal events, confirmed from the peak temperature (T_p), which corresponds to the point where the rate of mass variation of the sample is at maximum, observed in the DTG curve. According to Sánchez, Capote, and Carrilo [30] and Souza et al. [34], the thermal decomposition of lignocellulosic materials can be divided into four parts: loss of moisture, decomposition of hemicellulose, decomposition of cellulose, and decomposition of lignin.

The first thermal event, at around 48 °C, confirms the water evaporation. After this event, changes in the thermal decomposition process of the Buriti foam occur. A second thermal event, at around 280 °C, is related to depolymerization of hemicellulose [33–36,38], and a third, at around 356 °C, to cellulose and lignin degradation [33,35,38]. According to Lafond and Blanchet [4] and Ornaghi Júnior et al. [33], depolymerization of hemicellulose occurs in the range between 180–350 °C, the random cleavage of the glycosidic bond of cellulose between 275–350 °C and the degradation of lignin between 200–500 °C.

Similar results were found by Monteiro et al. [37] that also evaluated the thermal behavior of Buriti biofoam through thermogravimetric analysis. The TGA and DTG curves revealed evidence of moisture release and decomposition of the lignocellulosic structure of the biofoam. In this study, the material presented thermal stability up to 160 °C. According to the authors, this result indicates a characteristic for possible engineering applications of the Buriti biofoam.

The results on the thermal behavior of the Buriti foam suggest that, regarding thermal stability, the vegetable foam can be used as a building material, since the limit operating temperature of 180 °C covers most applications of the materials in civil construction at low and medium temperature.

3.4. Thermal Conductivity Test

Knowing the thermal properties of materials is of great importance when selecting them for thermal insulation purposes. The main parameter that expresses the thermal performance of insulating material is its thermal conductivity [28].

The temperature variation on the upper and lower surface of the samples during the experimental procedure are shown in Figure 10.

The temperature variation on the sample surfaces occurred as follows: a heating ramp, followed by a stable temperature level, and finally after the power supply was turned off, a cooling ramp.

Figure 10a shows the experiment carried out for the EPS sample, used as a comparative reference. Only the temperatures of the stable level, between 02:00 and 07:00 min, were accounted for. In this interval, the average temperature recorded by the thermocouple on the lower surface of the EPS sample was 51.47 °C. The average temperature measured by the thermocouple on the upper surface was 27.79 °C. When the power supply was turned off at approximately 07:40 min, the temperature in the thermocouple on the lower surface of EPS dropped sharply, matching the temperature recorded by the thermocouple on the upper surface at 25.1 °C.

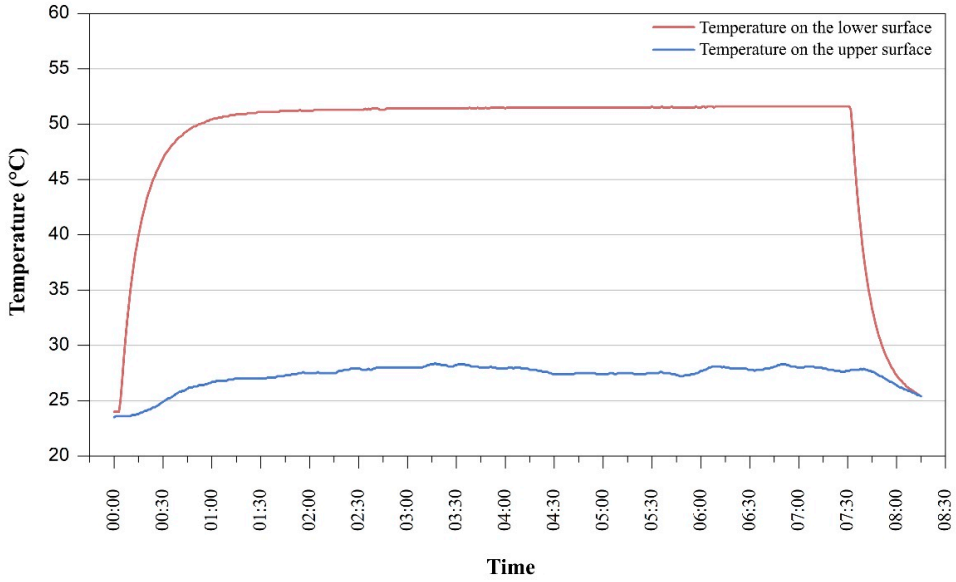

(**a**)

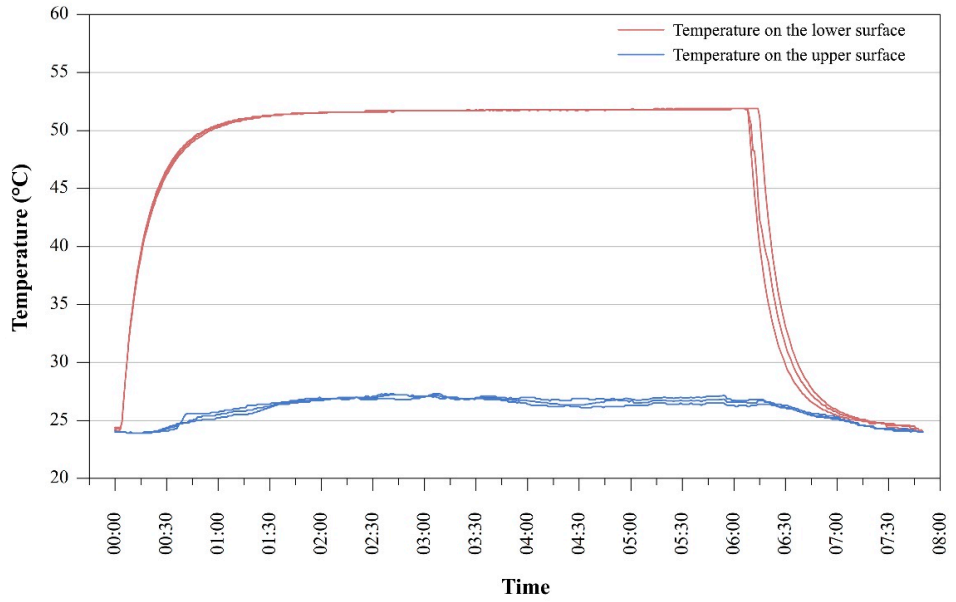

(**b**)

Figure 10. Temperature variation on the upper and lower surface of the samples: (**a**) EPS and (**b**) Buriti foam.

Through Equation (2) and the data shown in Table 4, the conduction heat flow (q_k) to the EPS sample was calculated at 198.91 W/m^2.

Table 4. Variables for measuring the conduction heat flow for the EPS sample.

Thermal Conductivity (λ)	Temperature Difference between Sample Surfaces (ΔT)	Thickness (L)
0.042 W/mK	23.68 °C	5 mm

Figure 10b shows the test performed on the three samples of the Buriti foam. The stable level of temperature considered in the calculations occurred between 02:00 and 06:00 min. During this time, the average temperatures recorded by the thermocouple on

the bottom surface of samples 1, 2, and 3 of the Buriti foam were 51.76 °C, 51.74 °C, and 51.75 °C, respectively.

On the upper surface of the vegetable foam, the average temperatures collected by the thermocouple in samples 1, 2, and 3 were, respectively, 26.59 °C, 26.88 °C, and 26.85 °C. This aspect showed a trend of better performance for thermal insulation of Buriti foam as the temperatures on the upper surface of the samples were at least 0.91 °C lower when compared to EPS, in the same condition.

After the power supply was turned off at about 06:10 min, the temperature on the bottom surface of the Buriti foam samples rapidly decreased until reaching the same temperature value recorded on the upper surface of the samples at approximately 24.2 °C.

Through the Fourier Conduction Law (see Equation (2)) and the data shown in Table 5, the value of the thermal conductivity coefficient (λ) experimentally measured for the Buriti foam was 0.0398 ± 0.0003 W/mK.

Table 5. Variables for measuring thermal conductivity for Buriti foam samples.

Samples	Temperature Difference between Sample Surfaces (ΔT)	Heat Flow (q_k)	Thickness (L)
Sample 1	25.17 °C	198.91 W/m^2	5 mm
Sample 2	24.86 °C		
Sample 3	24.90 °C		

According to Asdrubali, D'Alessandro, and Schiavoni [32], thermal insulators present conductivity lower than 0.07 W/mK. The low thermal conductivity of the Buriti foam can be explained by the cellular characteristic observed in the morphological analysis and by its low density. This happens because, in porous materials with thin walls, the presence of small, closed cells makes heat exchanges by convection negligible. Therefore, only conduction heat exchanges are important, but their effect is reduced considering the small solid fraction of the material and the low thermal conductivity of the air enclosed within the pores [31]. Moreover, solid materials with lower apparent density tend to have lower thermal conductivity [29].

Additionally, the measured value does not differ much from those obtained for conventional thermal insulation materials used in buildings such as rock wool, glass fiber, expanded polystyrene (EPS), and polyurethane foam (PUR), whose thermal conductivities generally range from 0.022 to 0.042 W/mK [28,32,39].

The need to develop new effective materials for thermal insulation and low environmental impact has led researchers to invest in this area [28]. Table 6 reports a comparison between the thermal conductivity of the Buriti foam with other materials of plant origin.

Table 6. Comparison of the thermal conductivity of the Buriti foam with other thermal insulating materials of plant origin.

Material	Thermal Conductivity (W/mK)	Apparent Density (kg/m^3)	References
Buriti Foam	0.0398 ± 0.0003	49.38 ± 5.9	Present Work
Hemp fiber	0.039–0.076	18–85	[5,40]
Date palm fiber	0.033–0.085	121–389	[5,10,28]
Sisal fiber	0.042–0.044	–	[39]
Coir fiber	0.040–0.055	75–125	[28,41]
Flax fiber	0.038–0.075	20–100	[5,28]
Oil palm fiber	0.055–0.091	20–120	[28,32]
Pineapple leaf fiber	0.035–0.043	178–232	[28,32]
Cane bagasse	0.046–0.055	70–350	[32,42]
Bamboo fiber	0.042–0.046	70–170	[43]
Jute	0.046–0.055	26–350	[5,28,32]
Cork	0.037–0.050	110–170	[28]

The thermal conductivity of the Buriti foam is in the same range as other thermal insulators of vegetable origin reported in the literature, many of which are already commercially available and in increasing use in built environments. Based on this, the Buriti foam can be argued as a viable thermal insulating material for application in buildings.

3.5. Sound Absorption Test

Sound absorption refers to the ability of some materials to reduce sound reflections within an enclosure. These materials are known as sound absorbers and can reduce the reverberation time and ensure sound intelligibility.

The sound absorption coefficients of the Buriti foam samples, in the longitudinal and transverse sections, are shown in Figure 11.

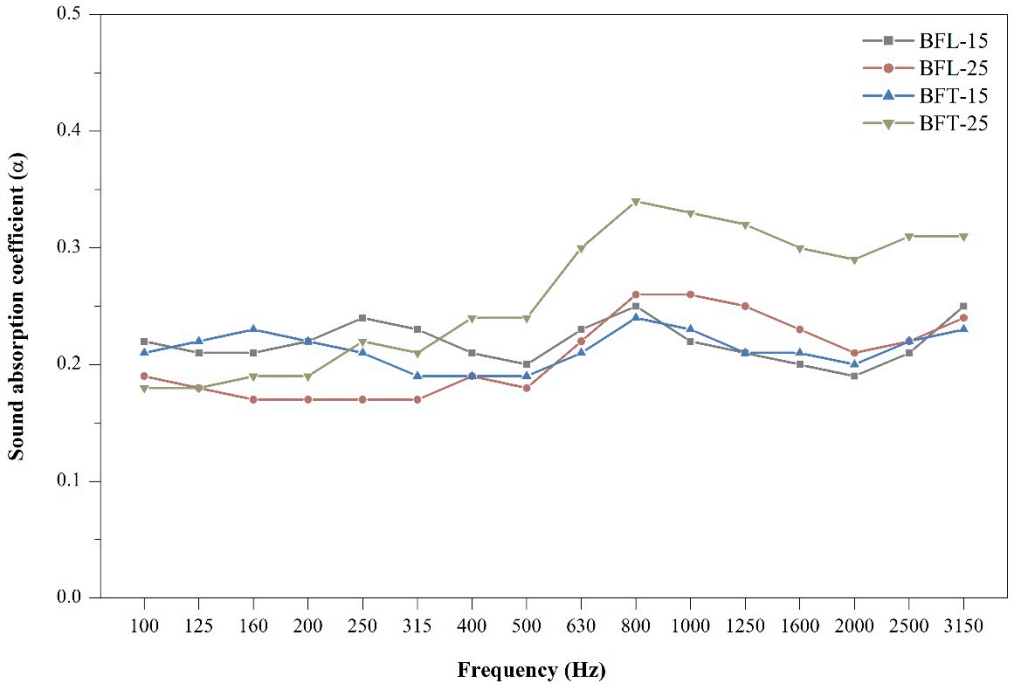

Figure 11. The sound absorption coefficient of Buriti foam samples.

In general, the sound absorption of the Buriti foam samples was discreet, ranging from 0.17 to 0.34 within the analyzed frequency range. This characteristic is mainly explained by the absence of open porosity in the material, as observed from the morphological analysis. According to Bakatovich et al. [6], in a porous material, the air can be contained in inclusions or connected to the surrounding environment. However, sound absorption is only improved when the material has a high open porosity and sufficient permeability.

With respect to longitudinally cut samples, the BFL-15 configuration has a sound absorption between 0.19 and 0.25 with a maximum value at 800 and 3150 Hz. As for the BFL-25 configuration, the sound absorption varies from 0.17 to 0.26 with a maximum value at 800 and 1000 Hz. It is noted that the BFL-25 configuration has sound absorption coefficients slightly higher than those of the BFL-15 configuration, between 800 and 2500 Hz. This demonstrates that the increase in thickness of the longitudinally cut Buriti foam samples slightly contributed to higher sound absorption values.

A more evident difference in the sound absorption profiles is seen for the configurations of the Buriti foam cut in the transverse direction. The BFT-15 configuration exhibits sound absorption between 0.19 and 0.24, reaching a higher value at 800 Hz. On the other hand, in the BFT-25 configuration, the sound absorption coefficients vary from 0.18 to 0.34, with a greater value also at 800 Hz. It is also verified that after 250 Hz, the BFT-25 configuration has higher sound absorption values when compared to the BFT-15 one. This

shows that the increase in thickness had a slightly more effective action on the sound absorption performance for the Buriti foam samples cut transversely.

Although one of the factors that influence the sound absorption of a material is thickness, this is more relevant at low and medium frequency ranges (100–2000 Hz), losing significance at high frequencies (>2000 Hz) [7,44,45]. That occurs because waves have a longer wavelength at lower frequencies, which means that thicker materials contribute to better sound absorption. It is imperative to note that the material's thickness should be approximately 10 to 25% of the wavelength and be in the recommended condition of lower frequencies (<2000 Hz) to act as a more effective sound absorber [44,45]. Materials with a thickness smaller than 30 mm are classified as thin sound absorbers, while materials with thickness greater than 30 mm are thick absorbers [7]. This explains the fact that the sound absorption of the samples of the configurations of greater thickness (25 mm) were not significantly greater than the samples of the configurations of a smaller thickness (15 mm) in the low and medium frequencies.

As the sound absorption coefficients depend on frequency, direct comparisons between materials cannot be easily performed for sound absorbers. On the other hand, sound absorption properties can also be defined through a single classification system, such as the Noise Reduction Coefficient (NRC), which is the arithmetic mean of the absorption coefficients measured in the 250, 500, 1000, and 2000 Hz bands, rounding the result to the nearest multiple of 0.05 [11,32,44,46]. This parameter is widely used commercially to represent the sound absorption performance of different acoustic materials and systems. Table 7 presents the NRC values for the Buriti foam samples.

Table 7. NRC of Buriti foam samples.

Sample Configuration	Frequency (Hz)				NRC
	250	500	1000	2000	
BFL-15	0.24	0.20	0.22	0.19	0.20
BFL-25	0.17	0.18	0.26	0.21	0.20
BFT-15	0.21	0.19	0.23	0.20	0.20
BFT-25	0.22	0.24	0.33	0.29	0.25

As can be seen, the BFT-25 configuration presents a slightly better sound absorption performance when compared to the other configurations, shown by its higher NRC value. Although the BFL-15, BFL-25, and BFT-15 configurations have the same NRC value, the use of this parameter has its limitations. Materials with the same NRC, do not necessarily have the same sound absorption performance [44]. It depends on the type of application and the condition of use of the material.

Any material is capable of absorbing sound, the difference is the sound absorption capacity that can be quite different. Materials with an NRC greater than 0.2 can be considered sound absorbers [29]. However, from a commercial point of view, good sound absorbers have NRC above 0.5. The NRC of conventional sound-absorbing materials used in buildings such as rock wool, glass wool, and polyurethane foam (PUR) reaches values up to 0.95 [47], 0.85 [47,48], and 0.65 [49], respectively.

Many studies, particularly on materials of plant origin, have been published presenting results from acoustic absorbers. Berardi and Iannace [3] analyzed the sound absorption behavior of fibers such as hemp, cane bagasse, coconut fiber, and cork. The results showed that these materials have good sound absorption coefficients, especially at medium and high frequencies. Arenas et al. [8] examined the absorption properties of esparto grass. The results of the sound absorption coefficients reported for some 90 mm thick samples reached a peak of sound absorption close to the unit at 500 Hz. Lim et al. [50] presented a study on the sound absorption characteristics of Kenaf fibers. They demonstrated that it had good sound absorption performance with a coefficient of 0.8 as of 1500 Hz for samples with a thickness of 40 mm. The authors reported that the result found corresponds to the sound absorption performance of conventional materials such as rock wool. Or, Putra

and Selamat [51] analyzed the sound absorption potential of oil palm fibers as an acoustic material. The samples with thicknesses of 40 mm showed high coefficients, of 0.9 on average, for frequencies above 1000 Hz.

Compared to the literature, Buriti foam shows lower performance than other materials of plant origin, displaying low sound absorption coefficients throughout the analyzed frequency range. However, the materials used in the comparison are made of fibers or granules, which are porous materials with interconnected cavities. These characteristics, which were not observed for Buriti foam, are needed to obtain good sound-absorbing materials.

Altogether, further studies are needed to understand the sound absorption mechanisms of the Buriti foam requires further studies. It is imperative to carry out new investigations, taking into account other forms of processing and other thicknesses of the material. The production of samples from the crushed vegetable foam can increase the open-air gaps as a way to improve the sound absorption performance of the material.

4. Conclusions

In this original and unprecedented research, the thermal insulation and sound absorption performance of Buriti foam were analyzed for potential application in buildings, thus contributing to the variety and sustainability of civil construction inputs. For this, analyzes were performed by scanning electron microscopy (SEM), apparent density, thermogravimetry (TGA and DTG), thermal conductivity, and sound absorption.

The SEM analysis showed a predominantly cellular morphology in the vegetable foam, with small and closed pores. As it is a porous and light material, the apparent density for the Buriti foam was 49.38 ± 5.9 kg/m^3. The thermal behavior by TGA and DTG demonstrated thermal stability of Buriti foam up to around 180 °C, which suggests the possibility of its use as a building material. It was possible to characterize the Buriti foam as an insulating material, with a thermal conductivity around 0.040 W/mK. The Buriti foam showed modest sound absorption values, from 0.17 to 0.34, throughout the analyzed frequency range, mainly due to the absence of open porosity in the material. The highest NRC for the analyzed samples was 0.25.

From these results, it can be concluded that the Buriti foam presents characteristics and potential for incorporation in buildings, mainly as ceiling boards, panels for thermal insulation of internal walls, filling of precast slabs, and monolithic wall panels. Future studies can be dedicated to evaluating and simulating the performance of the Buriti foam as a final product in constructive systems.

Author Contributions: Conceptualization, F.F.d.S.S., C.F.e.S. and L.C.C.N.; methodology, F.F.d.S.S., C.F.e.S., L.C.C.N.; software, F.F.d.S.S. and F.A.d.N.C.P.; validation, F.F.d.S.S., C.F.e.S. and L.C.C.N.; formal analysis, F.F.d.S.S., P.H.M. and C.F.e.S. and L.C.C.N.; investigation, F.F.d.S.S.; resources, F.F.d.S.S., R.L.C., F.A.d.N.C.P. and P.H.M.; data curation, F.F.d.S.S., R.L.C. and C.F.e.S.; writing—original draft preparation, F.F.d.S.S.; writing—review and editing, F.F.d.S.S., C.F.e.S., L.C.C.N, R.L.C. and P.H.M.; visualization, F.F.d.S.S., C.F.e.S., L.C.C.N., R.L.C.; supervision, C.F.e.S. and L.C.C.N.; project administration, F.F.d.S.S., C.F.e.S. and L.C.C.N. All authors have read and agreed to the published version of the manuscript.

Funding: This research received no external funding.

Data Availability Statement: The data presented in this study are available on request from the corresponding author.

Acknowledgments: The authors would like to thank the Graduate Program in Materials Science and Engineering of the Federal University of Piauí, the Graduate Program in Architecture and Urbanism of the University of Brasília, the Laboratory of Acoustics and Vibrations (LAVI) of the Federal University of Rio de Janeiro, the Zernike Institute for Advanced Materials of the University of Groningen, and the CNPq for the support in conducting this research.

Conflicts of Interest: The authors declare no conflict of interest.

References

1. Onésippe, C.; Passe-Coutrin, N.; Toro, F.; Desvasto, S.; Bilba, K.; Arsène, M. Sugar cane bagasse fibers reinforced cement composites: Thermal considerations. *Compos. Part A* **2010**, *41*, 49–556. [CrossRef]
2. Benmansour, N.; Agoudjil, B.; Gherabli, A.; Kareche, A.; Boudenne, A. Thermal and mechanical performance of natural mortar reinforced with date palm fibers for use as insulating materials in building. *Energy Build.* **2014**, *81*, 98–104. [CrossRef]
3. Berardi, U.; Iannace, G. Predicting the sound absorption of natural materials: Best-fit inverse laws for the acoustic impedance and the propagation constant. *Appl. Acoust.* **2017**, *115*, 131–138. [CrossRef]
4. Lafond, C.; Blanchet, P. Technical Performance Overview of Bio-Based Insulation Materials Compared to Expanded Polystyrene. *Buildings* **2020**, *10*, 9–16. [CrossRef]
5. Boukhattem, L.; Boumhaout, M.; Hamdi, H.; Benhamou, B.; Nouh, F.A. Moisture content influence on the thermal conductivity of insulating building materials made from date palm fibers mesh. *Constr. Build. Mater.* **2017**, *148*, 818–823. [CrossRef]
6. Bakatovich, A.; Davydenko, N.; Gaspar, F. Thermal insulating plates produced on the basis of vegetable agricultural waste. *Energy Build.* **2018**, *180*, 72–82. [CrossRef]
7. Yang, T.; Hu, L.; Xiong, X.; Petru, M.; Noman, M.T.; Mishra, R.; Militký, J. Sound Absorption Properties of Natural Fibers: A Review. *Sustainability* **2020**, *12*, 8477. [CrossRef]
8. Arenas, J.P.; del Rey, R.; Alba, J.; Oltra, R. Sound-Absorption Properties of Materials Made of Esparto Grass Fibers. *Sustainability* **2020**, *12*, 5533. [CrossRef]
9. Belhadj, B.; Bederina, M.; Makhloufi, Z.; Dheilly, R.M.; Montrelay, N.; Quéneudéc, M. Contribution to the development of a sand concrete lightened by the addition of barley straws. *Constr. Build. Mater.* **2016**, *113*, 513–522. [CrossRef]
10. Belakroum, R.; Gherfi, A.; Kadja, M.; Maalouf, C.; Lachi, M.; El Wakil, N.; Mai, T.H. Design and properties of a new sustainable construction material based on date palm fibers and lime. *Constr. Build. Mater.* **2018**, *184*, 330–343. [CrossRef]
11. Arenas, J.P.; Asdrubali, F. Eco-Materials with Noise Reduction Properties. In *Handbook of Ecomaterials*; Martínez, L., Kharissova, O., Kharisov, B., Eds.; Springer: Cham, Switzerland, 2018; pp. 1–26. [CrossRef]
12. del Rey, R.; Alba, J.; Rodríguez, J.C.; Bertó, L. Characterization of New Sustainable Acoustic Solutions in a Reduced Sized Transmission Chamber. *Buildings* **2019**, *9*, 60. [CrossRef]
13. Khalaf, Y.; El Hage, P.; Mihajlova, J.D.; Bergeret, A.; Lacroix, P.; El Hage, R. Influence of agricultural fibers size on mechanical and insulating properties of innovative chitosan-based insulators. *Constr. Build. Mater.* **2021**, *287*, 123071. [CrossRef]
14. Mrajji, O.; El Wazna, M.; Boussoualem, Y.; El Bouari, A.; Cherkaoui, O. Feather waste as a thermal insulation solution: Treatment, elaboration and characterization. *J. Ind. Text.* **2021**, *50*, 1674–1697. [CrossRef]
15. Caniato, M.; Cozzarini, L.; Schmid, C.; Gasparella, A. Acoustic and thermal characterization of a novel sustainable material incorporating recycled microplastic waste. *Sustain. Mater. Technol.* **2021**, *28*, e00274. [CrossRef]
16. Buratti, C.; Belloni, E.; Merli, F.; Zanella, V.; Robazza, P.; Cornaro, C. An innovative multilayer wall composed of natural materials: Experimental characterization of thermal properties and comparasion with other solutions. *Energy Procedia* **2018**, *148*, 892–899. [CrossRef]
17. Portela, T.G.R.; Costa, L.L.; Santos, N.S.S.; Lopes, F.P.D.; Monteiro, S.N. Tensile behavior of lignocellulosic fiber reinforced polymer composites: Part II buriti petiole/polyester. *Rev. Matéria* **2010**, *15*, 195–201. [CrossRef]
18. Karthik Babu, N.B.; Muthukumaran, S.; Arokiasamy, S.; Ramesh, T. Thermal and mechanical behavior of the coir powder filled polyester micro-composites. *J. Nat. Fibers* **2018**, *17*, 1058–1068. [CrossRef]
19. Santos, R.S.; Souza, A.A.; De Paoli, M.; Souza, C.M.L. Cardanol–formaldehyde thermoset composites reinforced with buriti fibers: Preparation and characterization. *Compos. Part A* **2010**, *41*, 1123–1129. [CrossRef]
20. Lorenzi, H.; Souza, H.M.; Costa, J.T.M.; Cerqueira, L.S.C.; Ferreira, E. *Palmeiras Brasileiras e Exóticas Cultivadas*; Plantarum: São Paulo, Brasil, 2004; p. 420.
21. Cattani, I.M.; Baruque-Ramos, J. Brazilian Buriti Palm Fiber (Mauritia flexuosa Mart.). In *Natural Fibres: Advances in Science and Technology towards Industrial Applications*; Fangueiro, R., Rana, S., Eds.; Springer: Dordrecht, The Netherlands, 2016; Volume 12, pp. 89–98. [CrossRef]
22. Sampaio, M.B.; Schmidt, I.B.; Figueiredo, I.B. Harvesting Effects and Population Ecology of the Buriti Palm (Mauritia flexuosa L. f., Arecaceae) in the Jalapão Region, Central Brazil. *Econ. Bot.* **2008**, *62*, 171–181. [CrossRef]
23. ASTM D1622. *Standard Test Method for Apparent Density of Rigid Cellular Plastics*; American Society for Testing and Materials: West Conshohocken, PA, USA, 2014.
24. Kreith, F.; Manglik, R.M.; Bohn, M.S. *Principles of Heat Transfer*, 7th ed.; Cengage Learning: Stamford, NY, USA, 2011.
25. ASTM E1050. *Standard Test Method for Impedance and Absorption of Acoustical Materials Using A Tube, Two Microphones and a Digital Frequency Analysis System*; American Society for Testing and Materials: West Conshohocken, PA, USA, 2012.
26. ISO 10534. *Acoustics—Determination of Sound Absorption Coefficient and Impedance in Impedance Tubes—Part 2: Transfer-Function Method*; International Organization for Standardization: Geneve, Switzerland, 1998.
27. Cardoso, M.S.; Gonçalez, J.C. Aproveitamento da casca do coco-verde (*Cocos nucifera* L.) para produção de polpa celulósica. *Ciência Florest.* **2016**, *26*, 330–331. [CrossRef]
28. Schiavoni, S.; D'Alessandro, F.; Bianchi, F.; Asdrubali, F. Insulation materials for the building sector: A review and comparative analysis. *Renew. Sustain. Energy Rev.* **2016**, *62*, 988–1011. [CrossRef]

29. Li, Y.; Ren, S. Acoustic and Thermal Insulating Materials. In *Building Decorative Materials*; Li, Y., Ren, S., Eds.; Woodhead Publishing: Shaxton, UK, 2011; pp. 359–374. [CrossRef]
30. Lavoratti, A.; Daiane, R.; Amico, S.C.; Zattera, A.J. Influence of fibre treatment on the characteristics of buriti and ramie polyester composites. *Polym. Polym. Compos.* **2017**, *25*, 818–823. [CrossRef]
31. Knapic, S.; Oliveira, V.; Machado, J.S.; Pereira, H. Cork as a building material: A review. *Eur. J. Wood Wood Prod.* **2016**, *74*, 775–791. [CrossRef]
32. Asdrubali, F.; D'Alessandro, F.; Schiavoni, S. A review of unconventional sustainable building insulation materials. *Sustain. Mater. Technol.* **2015**, *4*, 1–17. [CrossRef]
33. Ornaghi Júnior, H.L.; Moraes, A.G.O.; Poletto, M.; Zattera, A.J.; Amico, S.C. Chemical composition, tensile properties and structural characterization of buriti fiber. *Cellul. Chem. Technol.* **2016**, *50*, 15–22. Available online: https://www.cellulosechemtechnol.ro/pdf/CCT1(2016)/p.15-22.pdf (accessed on 3 November 2020).
34. Souza, S.A.V.; Silva, M.C.; Silva Júnior, O.G.; Mottin, A.C.; Oréfice, R.L.; Ayres, E. Design and characterization of bio-composites from poly (lactic acid) (pla) and buriti petiole (Mauritia flexuosa). *J. Renew. Mater.* **2017**, *5*, 251–257. [CrossRef]
35. Moura, A.S.; Demori, R.; Leão, R.M.; Frankenberg, C.L.C.; Santana, R.M.C. The influence of the coconut fiber treated as reinforcement in PHB (polyhydroxybutyrate) composites. *Mater. Today Commun.* **2019**, *18*, 191–198. [CrossRef]
36. Sánchez, M.L.; Capote, G.; Carrillo, J. Composites reinforced with guadua fibers: Physical and mechanical properties. *Constr. Build. Mater.* **2019**, *228*, 116749. [CrossRef]
37. Monteiro, S.N.; Rodriguez, R.J.S.; Costa, L.L.; Portela, T.G.R.; Santos, N.S.S. Thermal behavior of buriti biofoam. *Rev. Matéria* **2010**, *15*, 104–109. [CrossRef]
38. Martins, M.A.; Mattoso, L.H.C.; Pessoa, J.D.C. Comportamento térmico e caracterização morfológica das fibras de mesocarpo e caroço do açaí (Euterpe oleracea Mart.). *Rev. Bras. Frutic.* **2009**, *31*, 1150–1157. [CrossRef]
39. Neira, D.S.M.; Marinho, G.S. Nonwoven sisal fiber as thermal insulator material. *J. Nat. Fibers* **2009**, *6*, 115–126. [CrossRef]
40. Kosiński, P.; Brzyski, P.; Szewczyk, A.; Motacki, W. Thermal properties of raw hemp fiber as a loose fill insulation material. *J. Nat. Fibers* **2018**, *15*, 717–730. [CrossRef]
41. Damfeu, J.C.; Meukam, P.; Jannot, Y. Modeling and measuring of the thermal properties of insulating vegetable fibers by the asymmetrical hot plate method and the radial flux method: Kapok, coconut, groundnut shell fiber and rattan. *Thermochim. Acta* **2016**, *630*, 64–77. [CrossRef]
42. Asdrubali, F.; Ferracuti, B.; Lombardi, L.; Guattari, C.; Evangelisti, L.; Grazieschi, G. A review of structural, thermo-physical, acoustical, and environmental properties of wooden materials for building applications. *Build. Environ.* **2017**, *114*, 307–332. [CrossRef]
43. Huang, Z.; Sun, Y.; Musso, F. Hygrothermal performance of natural bamboo fiber and bamboo charcoal as local construction infills in building envelope. *Constr. Build. Mater.* **2018**, *177*, 342–357. [CrossRef]
44. António, J. Acoustic behavior of fibrous materials. In *Fibrous and Composite Materials for Civil Engineering Applications*; Fangueiro, R., Ed.; Woodhead Publishing: Shaxton, UK, 2011; pp. 306–324. [CrossRef]
45. Amares, S.; Sujatmika, E.; Hong, T.W.; Durairaj, R.; Hamid, H.S.H.B. A review: Characteristics of noise absorption material. *J. Phys. Conf. Ser.* **2017**, *908*, 012005. [CrossRef]
46. ASTM C423. *Standard Test Method for Sound Absorption and Sound Absorption Coefficients by the Reverberation Room Method*; American Society for Testing and Materials: West Conshohocken, PA, USA, 2017.
47. Lim, Z.Y.; Putra, A.; Nor, M.J.M.; Yaakob, M.Y. Sound absorption performance of natural kenaf fibres. *Appl. Acoust.* **2018**, *130*, 107–114. [CrossRef]
48. Yeon, J.; Kim, K. Analysis of Absorption Coefficient for Eco-Friendly Acoustical Absorbers. *Adv. Mater. Res.* **2013**, *831*, 58–61. [CrossRef]
49. Yeon, J.O.; Kim, K.; Yang, K.; Kim, J.; Kim, M. Physical properties of cellulose sound absorbers produced using recycled paper. *Constr. Build. Mater.* **2014**, *70*, 494–500. [CrossRef]
50. Chen, S.; Jiang, Y. The acoustic property study of polyurethane foam with addition of bamboo leaves particles. *Polym. Compos.* **2016**, *39*, 1370–1381. [CrossRef]
51. Or, K.H.; Putra, A.; Selamat, M.Z. Oil palm empty fruit bunch fibers as sustainable acoustic absorber. *Appl. Acoust.* **2017**, *119*, 9–16. [CrossRef]